Received: 19 February 2021 | Accepted: 25 January 2022

DOI: 10.1111/arcm.12758

ORIGINAL ARTICLE

Historical underground quarrying: A multidisciplinary research in the Caumont quarry (c. 13th–19th centuries), France

Daniel Ballesteros[1,2] | **Carole Nehme**[1] | **Bastien Roussel**[1] | **François Delisle**[3] | **Edwige Pons-Branchu**[4] | **Damase Mouralis**[1]

[1]UMR 6266 IDEES, Université of Rouen-Normandie/CNRS, Mont Saint-Aignan, France

[2]Departamento de Geodinámica, Universidad de Granada, Granada, Spain

[3]Laboratoire du GRHIS EA 3831, UFR des Lettres et Sciences Humaines, Université de Rouen-Normandie, Mont-Saint-Aignan, France

[4]Laboratoire des Sciences du Climat et de l'Environnement, LSCE/IPSL, CEA-CNRS-UVSQ, Université de Paris-Saclay, Gif-sur-Yvette, France

Correspondence
Daniel Ballesteros, UMR 6266 IDEES, Université of Rouen-Normandie/CNRS, Mont Saint-Aignan CEDEX, France.
Email: ballesteros@geol.uniovi.es

Abstract

Quarries represent 'landscapes archives' as they supplied the stone required for historical buildings. Among them, the Caumont ancient quarry stands out in northern France, with its huge dimensions and its historical role, providing building stones at a regional scale since at least the Middle Ages. The present study aims to approach the quarrying methods used over time in Caumont by means of an optimized methodological approach. The designed methodology combines (1) the 3D modelling of the quarry, (2) archaeological prospection, (3) stratigraphical and microscopical study of the quarried bedrock, and (4) the geochronological approach in stalagmites precipitated inside the quarry. The studied quarry of Caumont was excavated as an open-cast quarry beginning with the escarpments along the River Seine and transformed later to an underground quarry supported by contoured bedrock pillars. The underground quarry with its 12 km of galleries shows a chambers-and-pillars pattern style excavated using two methods, producing an inferred volume of 273,529 m^3 of building stone. The U–Th dating of two stalagmites suggests that quarrying activity had begun since at least the early medieval period and agrees with the excavation techniques and historical documents.

KEYWORDS

3D modelling, historical quarrying, multidisciplinary research, underground quarry

INTRODUCTION

Since Antiquity, quarries have played an important role providing stones for building because of the relative high compressive strength, durability and natural abundance of rocks (Klemm & Wiggins, 2016). Quarrying activity reflects the transformations of ancient societies, from sporadic works supplying local demands, to the development of an organized industry linked to technological progress (Djurić, 2019; Pivko, 2018; Storemyr & Heldal, 2017). Indeed, quarrying represents a powerful economic activity, frequently strategic and associated with many outstanding civilizations (Bevan & Bloxam, 2016; Fort et al., 2019; Zaid et al., 2015). The diffusion of building stones, whose provenance could be traced back to the quarries, is a powerful tool to establish ancient trade routes and the structuration of territories (Freccero, 2015; Shekofteh et al., 2020; Wilson & Bowman, 2018). Consequently, building stones represent valuable archaeomaterials and their related quarries can be considered as 'archives for past landscapes' (Bevan & Bloxam, 2016).

A historical review of underground quarrying is included in Supplementary Data 1. This activity was scarce throughout history compared to open-cast exploitations. Locally, the increased demand for suitable stone for construction and the scarcity of such material in natural outcrops promoted the development of underground quarries to continue exploiting laterally specific rocky volumes (Attanasio et al., 2015; Mileusnić et al., 2019; Storemyr & Heldal, 2017). Underground works implied additional engineering challenges related to groundwater and the stability of the galleries (Gao et al., 2019; Perrotti et al., 2019). Even though technical similarities exist between open-cast and underground quarries, particular techniques were applied to search for stable and cost-effective material (Mileusnić et al., 2019; Pivko, 2018; Rožič et al., 2018). Underground quarries usually exploited carbonate rocks since its relative high cementation favours the stability of excavation volumes, allowing the natural preservation of large, excavated galleries without any support structure (Gao et al., 2019; Scotto di Santolo et al., 2015).

Research conducted in ancient underground quarries focused mainly on the archaeological aspects of such ancient structures (Pivko, 2017; Storemyr & Heldal, 2017; Tziligkaki & Stamatakis, 2016). These studies combined a variety of methods such as the collection of historical documents (e.g., ancient pictures, maps) and the analysis of tool marks and inscriptions to define the excavation technique and geometry of the quarries. Archaeological studies were usually complemented by the geological characterization of the exploited stone via optical microscopy and geochemical analysis in order to trace the origins of dimensional stones used in landmark buildings (Attanasio et al., 2015; Brilli et al., 2018; Korkanç, 2018). All this data were compiled in a regional or a national database (Hyslop et al., 2010; Russell, 2017; Shawarby et al., 2009), sometimes using geographical information systems (Orbons, 2018; Turmel et al., 2016). In addition, quarries were investigated to assess the quality of the produced stone (De Kock et al., 2015; Korkanç, 2018) or the stability of the structure throughout geophysical investigations (Al Heib et al., 2015; Gao et al., 2019; Perrotti et al., 2019).

The technological knowledge of underground quarrying activity specifically for the medieval and modern periods is poorly investigated. Useful data such as rates of stone production and quantified volume of excavated stones remain difficult to reconstruct. Our study investigates a large ancient underground quarry with 12 km of galleries excavated since the medieval period. The quarry named Caumont and located in Normandy, northern France, had a regional relevance in the production of the Normandy chalkstone, a building stone designated as Global Heritage Stone Resource for its relevant historical role (Ballesteros et al., 2021). Our work aims to define the technological knowledge developed in Caumont quarry by reconstructing the excavation techniques and inferring production and excavation rates. For that, a multidisciplinary approach was conducted combining geomatics, archaeological, geological and geochronological techniques.

SETTINGS

The Seine valley has been extensively quarried with dozens of underground excavated galleries to supply building stone to Paris and surroundings areas of northern France since Roman times (Fronteau et al., 2010). Historical quarrying in the Caumont area is located between La Bouille and Mauny, on the south bank of the River Seine, 25 km southwest of Rouen (Figure 1). A huge volume of chalkstone was exported from this area to the buildings of the Seine Valley during the Middle Ages (Ballesteros et al., 2021) and following centuries, competing with other construction workshops in Caen, Vernon and Paris, among others (Dujardin, 2004, 2006). The quarried bedrock in Caumont corresponds to dedolomitized chalk, a singular coccolithic limestone of the Upper Cretaceous in age (Ballesteros et al., 2020, 2021). This quarrying area includes more than 10 exploitations (e.g., Caumont, Maquisards, Pylone, Jacqueline); the major one is specifically named Caumont quarry (Sibout, 2011; Tomat, 2009), the openings of which are located at 200 m from the River Seine (Figure 1b).

Historical works revealed that the Caumont quarrying area was active from the Middle Ages to 1906 CE, supplying stone for buildings located along the lower Seine valley (Dujardin, 2004, 2006; Lardin, 1998, 2016). Recently, geoarchaeological studies suggested that Caumont provided stones during the 10th–14th centuries, for buildings located 40 km away from the quarry site (Ballesteros et al., 2022). This provision area, larger than what is known

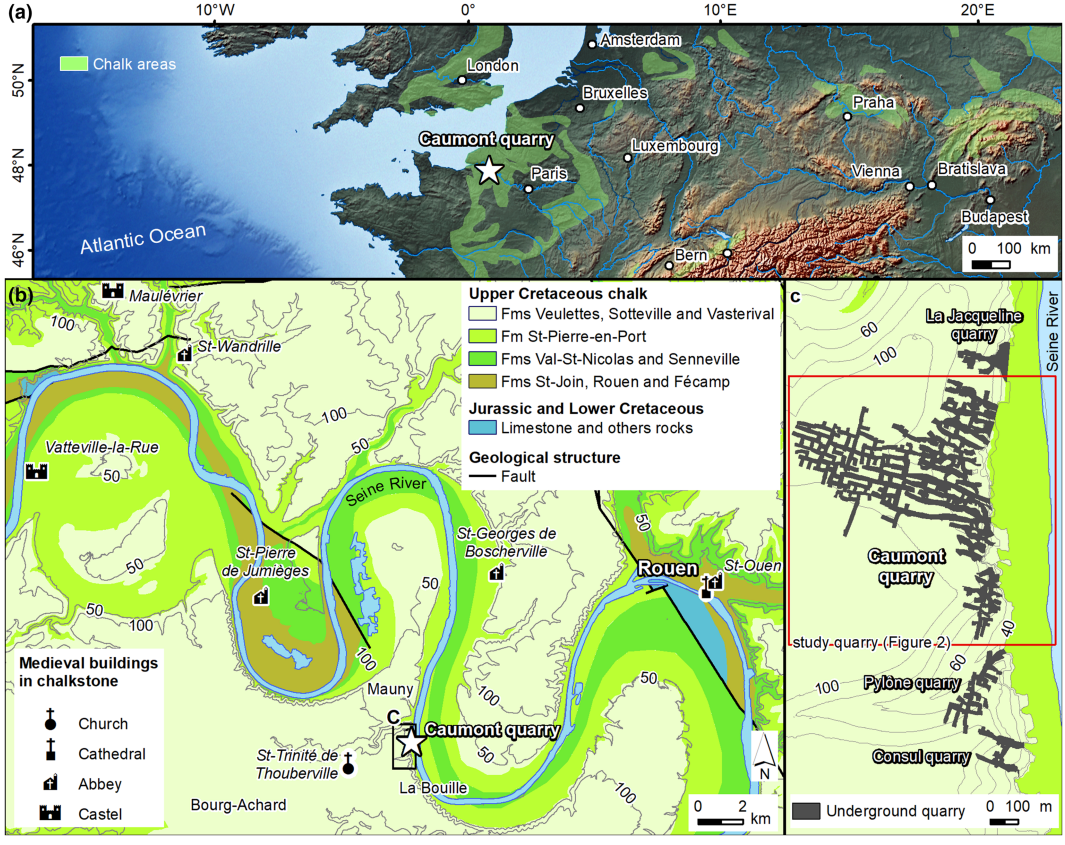

FIGURE 1 (a) Location of Caumont quarry in Western-Central Europe. (b) Geological map of the surroundings of Caumont quarry, showing geological formations (Fms) as defined in Lasseur et al. (2009). Geological data are after the Bureau de Recherches Géologiques et Minières (Quesnel et al., 2008; Van Lint et al., 2003). (c) Caumont quarry and other nearby underground exploitations [Color figure can be viewed at wileyonlinelibrary.com]

for medieval quarries, was facilitated by the fluvial mean of transport along the Seine. Coevally to the flourishing industrial activity of Caumont, the Duchy of Normandy was founded and expanded during the High and Late Middle Ages (Webber, 2005). The construction of remarkable buildings in Normandy as well as in England required supplying stone material provided by quarries such as Caumont.

METHODOLOGY

The multidisciplinary methodology combines geomatics and archaeological, geological and geochronological techniques (see Supplementary Data 2—Figure S2.1).

Geomatics

A 2D topographical survey and two 3D models of Caumont quarry were completed to create a base map of the quarry and to conduct a spatial analysis of the quarry geometry and excavation techniques. Open-cast and underground galleries were surveyed at a 1:200 scale based on 30 fixed stations located at the quarry entrances. Galleries were surveyed using the polyline method, carrying out 1629 stations and 1801 survey shots between stations. Each shot was measured by a calibrated Disto X2 device Trimmis (2018), processing 12,607 items of data in Compass software (Fish, 2001). Finally, the quarry mas was designed in ArcGIS, showing a global error estimated at $1.8 \pm 1.5\%$ considering the closing error and length of 109 closed survey polylines.

The quarry's volume was modelled at low and high resolution. The low-resolution 3D model includes the entire excavated galleries, providing a global vision and geometrical parameters defined in Supplementary Data 2—Table S2.1. This model resulted from the 2D survey and was constructed by jointing 1801 cuboids defined between survey stations in Compass (Fish, 2001). The high-resolution 3D model comprises only a part of the Caumont quarry system (Les Maquisards) and was completed to identify more specific techniques such as changing patterns in the exploitation system. Les Maquisards 3D model, forming 24% of the Caumont quarry system, was derived from 198 scanning stations acquired by means of the terrestrial laser scanner (TSL) FARO Focus M 70. Acquired point clouds were filtered, refined and assembled into a single cloud using the Trimble Realwork, and the subsequent closed triangulated model was elaborated at 10 mm precision using 3D Reshaper software.

Archaeological prospection

Archaeological evidence of the exploitation system in Caumont quarry comprises all the types of uses in an underground quarry, such as excavation structures and side rectangular galleries, toolmarks and unfinished works. All this evidence was represented in the quarry map and integrated in ArcGIS.

Geology

Geological analysis was conducted to characterize the quarried stone source to identify the ancient quarrying method. These analyses include geological mapping at a 1:1000 scale, elaboration of the stratigraphical section of exploited benches, microscopical analyses, (11 samples) and analyses of rock massif discontinuities (92 fractures and joints).

Geochronology

Two speleothems precipitated inside the underground galleries were dated by the $^{230}Th/^{234}U$ method to establish a maximum age for the quarry opening, as both speleothems were precipitated after the beginning of the excavations. Seven samples (70–270 mg) were taken respectively along the growth axis (different depths) of Maq speleothem (four samples) and CAU speleothem (three samples) using a micro drill and following the chemical preparation described in Pons-Branchu et al. (2014). U and Th were analysed on the Neptune Plus Plasma multi-collector inductively coupled plasma mass spectrometer installed at the LSCE/IPSL (Gif sur Yvette, France). For age correction (of ^{230}Th from the detrital contamination), two approaches were used: the first one is based on a fixed $^{230}Th/^{232}Th$ ratio for the detrital fraction, and the second one is based on the 'stratigraphical constraint' approach (Hellstrom, 2006). Here, the STRUTage routine (Roy-Barman & Pons-Branchu, 2016) was used for this correction.

Quarrying methods

The quarrying methods were reconstructed to characterize the underground quarrying developed in Caumont since the medieval period. The combination between the geological data, volume of galleries, excavation geometry and tool marks allowed us to extrapolate the rate and volume of stone production. The excavation of the flinty layers and other beds, as well as other works, generated waste deposits partially used for other applications, such as rubblestone employed for walls and foundations or for lime production (Ballesteros et al., 2021). The volume and production rate of the waste deposits can be also estimated considering the volume of the underground quarry, the stone production rate and a swell (or bulking) factor. The value of the swell factor would be 50% without compacting after waste accumulation in chalk bedrocks (Entwisle et al., 2015). Quarrying concepts and parameters are defined in Supplementary Data 2—Tables S2.1 and S2.2.

RESULTS

The geometry of the quarry

The Caumont quarry system comprises open-cast exploitations and an orthogonal network of 12 km of galleries located 110 m below the plateau surface (Figures 2 and 3). According to the 3D modelling, the floor surface of the underground quarry is ~212,648 m^2 (Table 1), which 80% correspond to galleries of 12–15 m wide and up to 8 m height. The remaining 20% represents the extension of three open-cast exploitations (Figure 2a). The quarry volume is ~1,655,940 m^3 (Table 1). 78% of the volume corresponds to the galleries and 22% to open-cast cuttings. In the galleries, the volume of the excavated rock per meter advanced by the exploitation front (specific volume) is ~108 m^3 each.

The Caumont quarry is divided in two sectors named A and B (Figure 2; see also quarry pictures in Supplementary Data 2—Figure S2.2). Sector A corresponds to the central and eastern parts of the quarry and includes all the entrances, four of them blocked by rock fall deposits. Sector A comprises galleries of 400 m long and N 110–120° E direction, interconnected by smaller galleries of N 10–20° E direction. This geometrical configuration generated rectangular pillars of 20–30 m wide and up to 285 m long. Two types of galleries are recognized in sector A: main galleries and contouring galleries.

The main galleries correspond to passages of 15 m wide and 8 m height. At the entrances of the quarry, the ceilings and walls of the main galleries are weathered and sometimes enlarged or

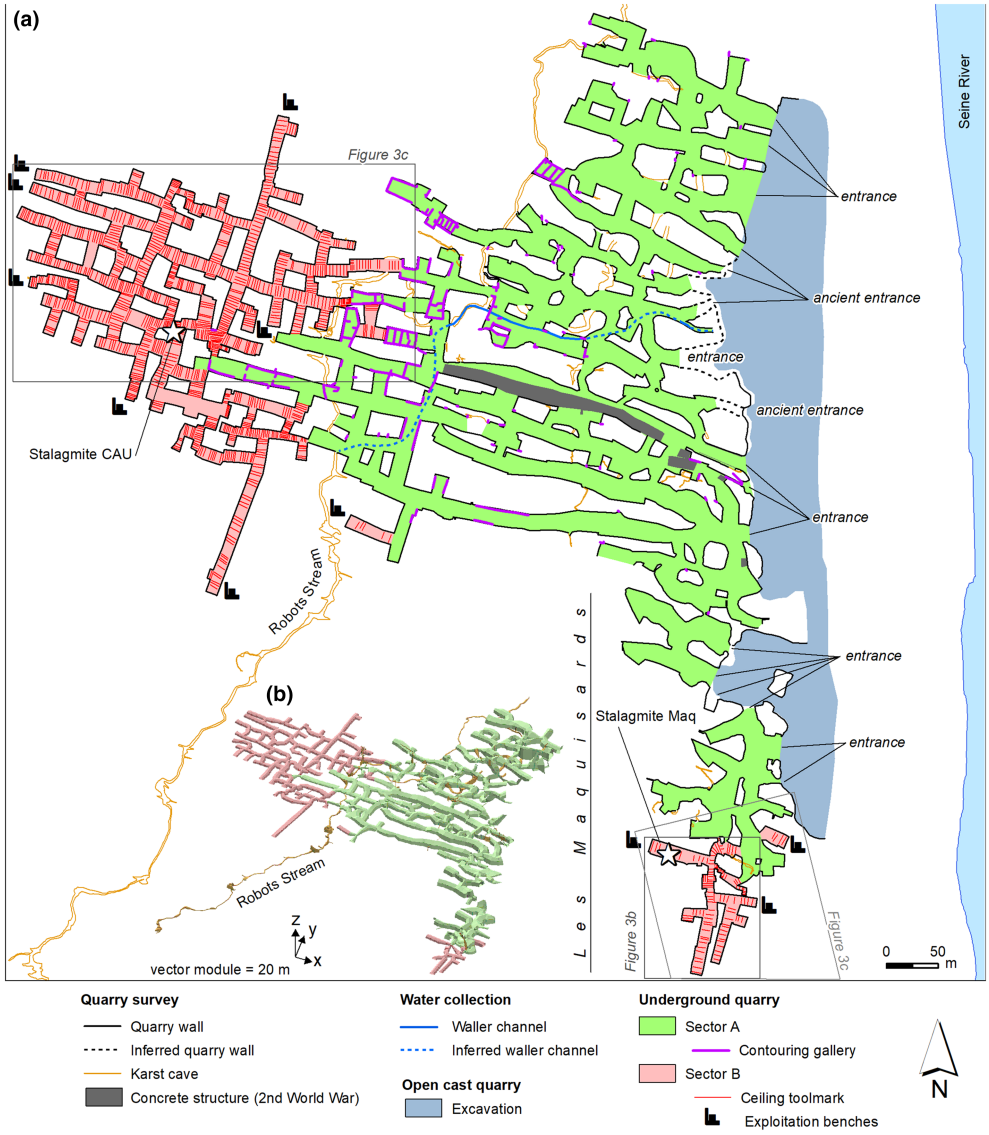

FIGURE 2 (a) Map of the Caumont quarry showing the open-cast area and the underground sectors A and B, as well as the intercepted karst caves studied by Nehme et al. (2020). The map resulted from the 2D topographical survey of que quarry. (b) Low-resolution 3D model of Caumont underground quarry [Color figure can be viewed at wileyonlinelibrary.com]

partially closed by rock fall processes. Waste deposits up to 7 m thickness cover the floor. The contouring galleries (e.g., *sapes de contournement* in French) (Figure 2) present rectangular sections of 0.5 m wide and 2 m height and are in two specific locations. The first is at the upper corners of the main galleries and parallel to the development of these galleries. Parallel contouring galleries are well preserved in the unfinished exploitation fronts as well at the top of the main galleries. The second location is perpendicular to the axes of the main galleries, as shown along the ceiling.

Sector B is located at the Western and deepest part of the quarry (Figure 2), hence this sector is younger than sector A. It comprises well-preserved cuboid-like galleries of 12 m wide and 5 m height, displaying exploitation benches at the end. This sector forms a network of cuboid-like galleries (<200 m) with N 100–110°E direction, while others are longer, with an N10–20°E

FIGURE 3 (a) West part of the quarry map showing ceiling toolmarks, excavation progress and examples of exploitation phases and corners. (b) Ceiling toolmarks shown by the high-resolution 3D model, indicating the direction of the exploitation in Les Maquisards part. (c) 3D geometry of the galleries. The starting points of sector B are indicated (white dots) in the three sections, the positions of which are shown in Figure 2A [Color figure can be viewed at wileyonlinelibrary.com]

direction (Figure 2a). The galleries are interconnected each 20–30 m, forming rectangular unquarried pillars of 10–30 m wide. The ceilings and floors are respectively 1 and 4 m higher than the galleries of sector A. Waste deposits of <2 m thickness cover the floor of sector B.

Exploitation benches, toolmarks and groundwater collection system

In sector B, the exploitation fronts located at the end of cuboid-like galleries (Figure 2a) comprise four frontal stepped benches, each of 1 m height (exploitation benches are documented in

TABLE 1 Geometrical parameters of the Caumont quarry derived from a low-resolution 3D model. Calculations and parameters are detailed in Supplementary Data 2—Table S2.1. The thickness of waste deposits is based on field survey

Parameter	Units	Complete quarry	Open-cast quarry	Underground quarry		
				Entire	Sector A	Sector B
Type of works	–	–	Open cast works	–	Main galleries Contouring galleries	Cuboid galleries with stairs-shaped benches
Quarry area	m^2	212,648	41,510	171,138	126,818	44,320
Quarry volume	m^3	1,655,940	357,650	1,298,290	1,091,069	207,221
Underground galleries						
Quarry specific volume	$m^3\ m^{-1}$	–	–	108	133	54
Quarry length	m	–	–	12,024	8,199	3,825
Gallery main orientations	Deg.	–	–	N 110–120° E N 10–20° E	N 110–120° E N 10–20° E	N 100–110° E N 10–20° E
Gallery average diameter	m	–	–	10.4	11.7	7.3
Gallery average width	m	–	–	13.5	15.3	11.6
Gallery average height	m	–	–	5.1	7.9	4.6
Gallery ceiling altitude	m	–	–	19	19	20
Gallery floor altitude	m	–	–	12	11	15
Gallery wall surface	m^2	–	–	505,537	426,089	79,448
Waste deposits inferred thickness	m	–	<15	–	<7	<2

Supplementary Data 2—Figure S2.2). Note that the stepped benches represent unfinished works just below the sheet flint. Other features such as vertical trenches exploited laterally were sometimes identified. The preserved cuts indicate that the benches were usually exploited from the top to the bottom and from the right to the left. Occasionally, extracted stones of 1 m wide were stored or abandoned inside the quarry and were later covered by precipitated calcite layers. The karst caves (Figure 2; Nehme et al., 2020) discovered during the excavation might have hampered the quarrying activity.

Toolmarks were identified in the underground galleries and documented (toolmarks are detailed in Supplementary Data 2—Table S2.3 and Figure S2.3). The walls in sector A preserve some marks caused by iron peaks, especially in the contouring galleries, where homogeneous marks due to chisels are very common. In sector B, the walls and the front of the exploitation benches show marks related to the impact of a lance (iron bars of ~1 m long), as described in Sibout (2011). The ceiling of the cuboid-like galleries shows horizontal marks due to a lance. These toolmarks have an asymmetric profile showing a clear direction of the excavations in sector B. The frontal excavation exploited, first, galleries towards the northwest and, second, towards the southwestern and northeastern parts (Figure 3a). As for the lateral excavation pattern, toolmarks are identified in the 3D model and related to lateral excavation of the longitudinal galleries, forming additional small corners (Figure 3b,c).

Archaeological remains include a water collection system that derived the groundwater of the Robots stream (see Supplementary Data 2—Figure S2.4). The collection system includes a water channel and an aqueduct. The water channel is made of wood with small iron bars. The preserved part of the channel is 155 m long, crossing the quarry galleries and karst caves. The total length of the structure is estimated to be 470 m. The aqueduct is made mainly of two stone walls. Other non-preserved parts would have been made of wood. The water system drained the water from the major cave conduit named Robots stream.

Geology

Stratigraphy of the quarried bedrock

The lower Coniacian chalk limestone, with many hardgrounds, flint nodules and sheet flints, was mainly exploited (a stratigraphical section and microscopical analyses of the quarried bedrock are shown in Supplementary Data 2—Figures S2.5, S2.6 and S2.7). Hardgrounds are reddish or greenish beds, cemented by carbonates, oxides and/or phosphates and, frequently, affected by bioturbation (Mortimore, 2011). Two hardgrounds have regional extension, named Belval and Epivent in Normandy (Hoyez, 2008), and Cliff and Hope hardgrounds in England (Mortimore, 2019). Flint nodules of 2–20 cm in diameter are concentrated in eight stratified beds of 10–20 cm thickness interbedded in the chalk strata. The sheet flint is a continuous layer, usually parallel to the bedding, formed by 2–5 cm of the Hope Gap flint (Mortimore, 2019). Hope Gap Sheet flint is located in the upper part of the quarry galleries and is sometimes divided into two sheet flints separated by less than 1 m.

Caumont chalkstone is a homogeneous white limestone classified as a dedolomitized biomicrite made of 5–40% micrite and comprising nanoscopic fragments of coccoliths, 5–40% of rhombohedral moulds, 5–25% of bioclasts and less than 5% of Mn–Ti–Fe oxides. Rhombohedral moulds are voids of 10–200 μm in size derived from the dissolution of crystals of dolomite formed during diagenesis. Sometimes, the moulds are filled with calcite. Bioclasts are fragments of echinoderms, calcispheres and foraminifers, the abundance of which increases in the upper and lower parts of the exploited strata. Some bioclasts of bryozoans, bivalves and gastropods can be identified under the optical microscope.

The combination of historical documents, field survey and petrology enables a correlation between the stratigraphical section and the exploited beds. Stratified flint nodules are separated by 0.4–1 m and mark the limits of the exploited beds. The latter are located below the sheet flint at the top of the galleries. This sheet flint was probably used as a guiding layer during stone extraction since it is located on the ceiling of sector A.

Petrophysical and mechanical properties are summarized in Ballesteros et al. (2021). The stone material with the highest mechanical quality corresponds to the Gros Lien bed as a result of its relative high values of hardness, penetration resistance and compression strength. Indeed, the Gros Lien bed shows abundant rhombohedral moulds filled by calcite related to the development of hardgrounds during chalk diagenesis. Consequently, the occurrence of hardgrounds (detailed in Ballesteros et al., 2020) explains the quality of the Caumont chalkstone as a historical construction material.

Massif rock discontinuities

The bedding is the main bedrock discontinuity and dips 2–3° to the southwest, describing a gentle fold, the axis of which is located more to the northeast. Fractures and joints constitute two

subvertical and orthogonal systems following N 40–50° E and 130–160° E directions (see rose diagram analyses in Supplementary Data S2—Figure S2.8). Fractures are dozens of metres long, showing less than 3 m of apparent displacements with normal or inverse components. Fractures are usually separated every 50–100 m and open (1–4 cm wide), sometimes with carbonate mineralization and detrital infills. The joints present 30–70° dipping and less than 10 m in length.

Clearly, underground galleries follow generally the subhorizontal bedding in order to exploit selected chalk strata. However, the main orientations of the galleries (N 10–20° E and N 100–120° E) are slightly different from the directions (N 30–50° E and N 140–160° E) of the two families of fractures and joints. Such configuration in Caumont avoided the exploitation of galleries following the two fractures and joint families, which constitutes an unfavourable situation for the stability of galleries. Galleries following the fractures and joints systems were subject to collapses and rock fall processes in underground excavations (Bieniawski, 1989; Romana, 1993).

Geochronology

$^{238}U/^{230}Th$, $^{234}U/^{238}U$ (expressed as $\delta^{234}U$), $^{230}Th/^{232}Th$ activity ratios, raw and corrected ages are reported in Supplementary Data 2—Table S2.4. U content ranges from 0.176 ± 0.001 to 0.420 ± 0.003 ppm, with ^{232}Th between 0.318 ± 0.003 and 27.2 ± 0.2 ppb. U isotopic activity is close to equilibrium with $\delta^{234}U \sim 100$ for CAU speleothem and ~ 200 for Maq stalagmite. All samples show low $^{230}Th/^{232}Th$ ratios, indicating an important proportion of detrital Th, and the need for age corrections.

Corrected ages (using STRUTages routine, see Roy-Barman & Pons-Branchu, 2016) ranging from 154 years (1865 CE) + 300/−145 and 800 years (1,219 CE) + 458/−482 years were determined for Maq speleothem and between 45 (1974 CE) + 55/−40 years and 112 (1907 CE) + 67/−59 years for CAU speleothem. Initial $^{230}Th/^{232}Th$ rate for the detrital fraction determined by STRUTages model was 1.24 ± 0.11 for CAU and 1.26 ± 0.04 for Maq speleothem, suggesting a common geochemical mechanism for element transfer from the surface to the quarry for both speleothems. Maq indicates a basal age of 1219 CE +458/−482 years. Even though the age uncertainties are high, the proposed period of growth for the Maq is in agreement with possible growth start during the medieval period.

DISCUSSION

Quarrying system

The exploitation of the chalk limestone in Caumont commenced at the basal part of the natural cliffs along the River Seine. The excavation was mainly open air, as shown in many scarps. The open-air exploitation turned later into an underground quarrying activity by drift mining, leaving large amounts of dismantled rocks and bulky waste deposits outside the present-day Caumont galleries. Underground quarrying was performed using two methods, A and B, which are related to sectors A and B, respectively.

Underground quarrying method A

This characterized method combines contouring structures and undermining excavations to cut and extract outward a large block. Method A is divided into six phases (Figure 4a):

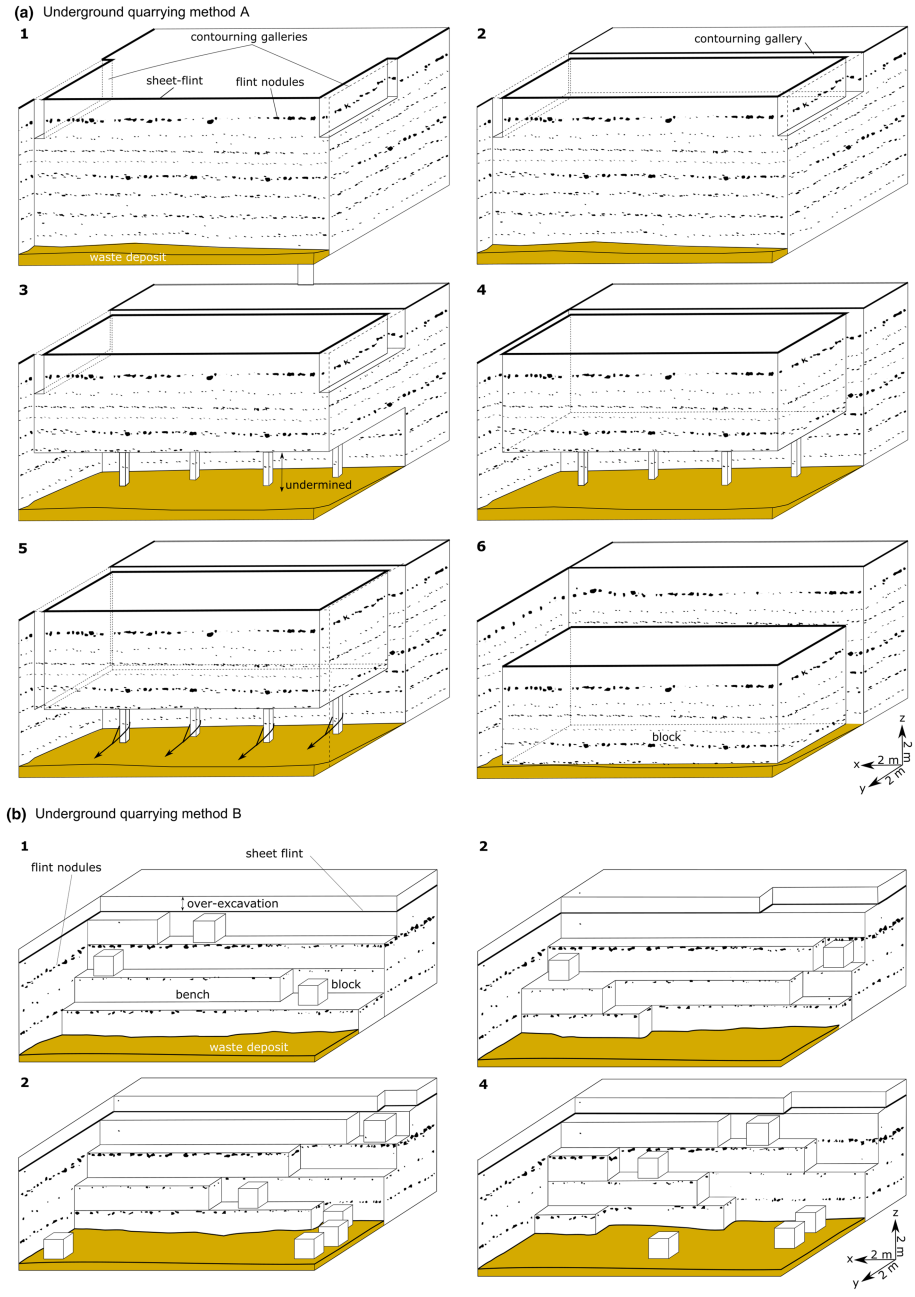

FIGURE 4 Reconstruction of the excavation method used in Caumont underground quarry. (a) Method A: (1) excavation of contouring galleries in the lateral and top of the exploitation front; (2) connection of the former contouring galleries; (3) undermining of the exploitation front, leaving small bedrock pillars and/or constructing columns in wood or chalkstone to support the excavation; (4) enlargement downwards of the contouring galleries; (5) removal of the small pillars; and (6) falling of a large block that can be reduced to smaller blocks. (b) Method B by the development of four stepped benches below the sheet flint; after over-excavation of the top of the exploitation front, benches were exploited from the top to the bottom and, probably, from the right to the left. Probable structures in wood are not represented in either method [Color figure can be viewed at wileyonlinelibrary.com]

1. The operation starts excavating two contouring galleries 4 m long in the upper corners of the exploitation front, parallel to the axis of the main gallery. Both galleries are usually straight and allow us to guide each operation, to explore the bedrock and detect damaging fractures and natural caves.
2. A new contouring gallery is then excavated from the end of previous contouring galleries, perpendicular to the axis of the main gallery, in order to join both contouring galleries.
3. The lower part of the exploitation front is excavated to create a void and extract a large block. Evidence of such undermining excavation is recognized in the unfinished works located in sector A. The undermined excavation would be supported by small pillars and/or small wooden or chalkstone columns.
4. The contouring galleries are enlarged downwards to detach the individual large rock block of 9 m wide, 8 m height and 3 m long.
5. The small pillars are then removed.
6. The large block falls to the floor. A wooden structure is then installed underneath to facilitate later works and block transport. Later, the individualized large block is reduced to smaller blocks.

Underground quarrying method B

Quarrying method A was later followed by method B with the development of new techniques related to the exploitation of benches (Figure 4b). This change from method A to B is well marked in the limit between sectors A and B, by a 1 m abrupt elevation of the ceiling. Method B consists of excavating stepped four benches of 1 m height and ~12 m width, located below the sheet flint. The exploitation begins with over-excavating 1 m strata above the sheet flint to cut off the uppermost bench. This over-excavation technique does not produce any dimensioned stone. Later, the benches are quarried from top to bottom and, possibly, from right to left, performing cuts in all three dimensions to obtain cuboid blocks of 1 m width, 0.7–1 m height and 0.5 m length.

Stone and waste deposit production

In sector A, the stone production rate was estimated to be ~19%, since method A involves the development of contouring galleries (0.5 m width, 2 m height) and undermined excavations (15 m width, 2 m height), which represent an unproductive volume of limestone turned into waste (Table 2). Later, the development of exploitation benches (method B) in sector B

TABLE 2 Inferred volumes of produced dimension stone and waste deposits in the Caumont underground quarry based on the quarry volumes and surface (Table 1). Values show an error of 5% according to the DISTOX precision (1.8 ± 1.5%) and 3D modelling via compass. Calculations procedures are detailed in Supplementary Data 2—Table S2.5

Parameters	Rate (%)	Volume (m^3)	Rate (%)	Volume (m^3)	Volume (m^3)
Sector	Sector A		Sector B		Overall
Stone production	19	210,956	30	62,570	273,529
Waste deposit production	81	1,320,169	70	216,976	1,537,145
Preserved waste deposit	38	507,272	31	66,480	573,752
Recycling rate of waste deposits	62	812,897	69	150,496	963,393

increased the production rate up to ~30%, because the unproductive volume of limestone turned into waste corresponds only to over-excavations (12 m width, 1 m height), carried out at the top of the exploitation front (cf. section 5.1.2). In total, the volume of the building stone produced during the time was estimated at 273,529 m^3 (Table 2).

Underground quarrying also generated waste deposits. The production rate of such waste was ~81% for sector A and ~70% for sector B (Table 2). In the overall volume of the waste deposits, the volume of the produced waste deposits (1,537,145 m^3) was much larger than the volume of the waste deposits preserved in the underground quarry (573,752 m^3). Such a difference might indicate that 59–67% of the produced waste deposits could have been recycled for other applications. In fact, the occurrence of excavations scarps in the waste deposits shows that waste deposits might have been exploited.

Technological knowledge of underground quarrying in Caumont

The Caumont underground quarry shows a regular geometry and relative uniform toolmarks, especially in sector B, as resulting from the use of two systematic quarrying methods. Method A combined systematic contouring galleries and undermined excavations to individualize a large chalk bedrock, whereas method B used regular exploitation benches. Additionally, both methods were aimed at selected strata and considered the stability of the quarry and the evacuation of water. The stone was extracted, specifically by quarrying 7 m of strata located below the Hope Gap sheet flint, which played a guiding role in the excavation. Regarding quarry stability, the galleries were excavated diagonally to the main fracture systems to prevent collapses and rock fall processes in ceiling and walls. Besides, the dimensions of the galleries were reduced in sector B, with more regular pillars than in sector A. Such structures would have increased the stability of sector B, compared to previous works. The groundwater was collected and evacuated through a suitable system of channels and aqueducts. Such structures and constructions left inside the galleries indicate that the quarrying activity in Caumont was carefully planned, considering the technological advances of each time period as well as the geological settings (e.g., stone extraction, stability of the galleries).

The specialization of the quarrying procedures in Caumont allowed the excavation of a massive underground quarry from the early medieval period to the beginning of the 20th century. The overall surface of Caumont quarry system (>60,000 m^2) is twice as large as the extension of both Chinese and Middle Eastern largest underground caverns, dated back from the Bronze Age to Antiquity (Gao et al., 2019; He et al., 2016). In general, the geometry of Caumont galleries is more regular and uniform than other exploitations dating back to Antiquity (Frumkin et al., 2014; Shtober-Zisu & Zissu, 2018), and resulted in systematic and standardized quarrying procedures employed in Caumont during the Middle Ages.

The quarrying methods evolved in time to increase stone production, the apparent recycling of waste deposits and, consequently, the profitability of stone extraction. Stone production rates increased from ~19% in sector A to ~30% in sector B. The Caumont production rates are still close to the rates (~25%) estimated in other historical underground quarries (Attanasio et al., 2015).

CONCLUSIONS

This study proposes a multidisciplinary approach to apply geomatics, archaeological and geological prospection and geochronological dating for studying historical underground quarrying. The Caumont quarry is the largest underground quarry in chalk limestone according to the

stone production and was chosen as a case study because of the geoheritage significance of such a site for Normandy. The geometry of the quarry defined by the 2D survey, the 3D model and geometrical parameters, combined with the identification of archaeological tools and marks, helped to characterize the quarrying methods used on site and set the technological knowledge of underground chalkstone quarries.

The geological analysis comprises the stratigraphy, petrology and fracturing network to identify the quarried strata. The additional microscopical study characterized the rock adequacy as a construction stone resource. The relationships between the geometry of the galleries and the fracture systems evaluate the stability of the quarry as a relevant factor in underground environments. This multidisciplinary research helped estimate the stone production rates and volumes for each identified quarrying method. Finally, the U–Th datings in stalagmites precipitated after the opening of the quarry constrained the chronology of the ancient quarry.

The Caumont underground quarry was excavated to obtain the Normandy dedolomitized chalkstone for buildings. Seven metres of chalk strata were laterally exploited by two methods, creating a network of 12 km of orthogonal galleries with bedrock pillars. The quarrying of both sectors A and B would have started during early medieval times, ending the activity in sector B at the beginning of the 20th century. Method A combined contouring galleries and undermined excavation to individualize large blocks from the bedrock. This method generates large and subparallel galleries forming the current sector A of the quarry, affected largely by rockfall and collapse processes. Later, method B was employed by the systematic development of more regular and smaller galleries with bedrock pillars and four exploitation benches. This change in quarrying technique implied a better planning of the quarry operations, strengthened the workforce to reduce instabilities issues and increased the stone production rate from ~19% to ~30%. Ultimately, the regular geometry of the underground galleries and the systematic quarrying methods adapted to the local geology indicates that the Caumont quarrying industry followed a well-designed plan resulting from the technological and geological knowledge of the medieval period.

ACKNOWLEDGEMENTS

We thank A. Painchault, M. Varano and D. Todisco (Université de Rouen-Normandie) for assistance, facilities and management of the archaeological investigation permission. We are also grateful to A. Farrant (British Geological Survey) and B. Hoyez (Université de Le Havre-Normandie) for his help in understanding the Chalk Group Stratigraphy and to M. Cueto (IDOM) for geotechnical advice. Finally, we acknowledge the Federation Française de Spéléologie and the Comité Régional de Spéléologie de Normandie, especially P. Rabelle, for assistance during fieldwork.

FUNDING INFORMATION

This research was undertaken under both *Archéomatériaux Territoie et Patrimoine* (ATP) and PALéoenvironnements et ECOsystèmes NORmands (PALECONOR) RIN projects, funded by Région Normandie.

AUTHOR CONTRIBUTIONS

DM and CN conceived and conducted the research and performed funding acquisition. DB carried out the quarry map, low-resolution 3D model and the geological study, defining also the ancient quarrying systems. BR and FD elaborated the high-resolution 3D model under the supervision of CN, who worked with EPB to obtain U–Th datings. DM carried out project administration. Finally, DB and CN wrote the original draft, with contributions from DM and EPB to the discussion and final version.

PEER REVIEW

The peer review history for this article is available at https://publons.com/publon/10.1111/arcm.12758.

DATA AVAILABILITY STATEMENT

Data available in article supplementary material

ORCID

Daniel Ballesteros https://orcid.org/0000-0002-2703-7730
Carole Nehme https://orcid.org/0000-0003-0004-0910
Bastien Roussel https://orcid.org/0000-0002-8292-2898
Edwige Pons-Branchu https://orcid.org/0000-0002-7941-3144
Damase Mouralis https://orcid.org/0000-0001-7748-0258

REFERENCES

Al Heib, M., Duval, C., Theoleyre, F., Watelet, J. M., & Gombert, P. (2015). Analysis of the historical collapse of an abandoned underground chalk mine in 1961 in Clamart (Paris, France). *Bulletin of Engineering Geology and the Environment*, *74*, 1001–1018. https://doi.org/10.1007/s10064-014-0677-6

Attanasio, D., Bruno, M., Prochaska, W., & Yavuz, A. B. (2015). A multi-method database of the black and white marbles of Göktepe (Aphrodisias), including isotopic, EPR, trace and petrographic data. *Archaeometry*, *57*, 217–245. https://doi.org/10.1111/arcm.12076

Ballesteros, D., Farrant, A., Nehme, C., Todisco, D., Woods, M., & Mouralis, D. (2020). Stratigraphical influence on chalk cave development in upper Normandy, France: Implications for chalk hydrogeology. *International Journal of Speleology*, *49*(3), 187–208. https://doi.org/10.5038/1827-806X.49.3.2319

Ballesteros, D., Painchault, A., Nehme, C., Todisco, D., Varano, M., & Mouralis, D. (2021). Normandy chalkstone (France): Geology and historical uses from quarries to monuments. *Episodes*, *44*, 1–42. https://doi.org/10.18814/epiiugs/2020/0200s03

Ballesteros, D., Painchault, A., Puente-Berdasco, B., Nehme, C., Todisco, D., & García-Alonso, J. I. (2022). Sourcing of chalkstone used in medieval buildings in the eastern Duchy of Normandy (10th–14th centuries) through geological and geochemistry analyses. *Geoarcheology* (accepted).

Bevan, A., & Bloxam, E. (2016). Stonemasons and craft mobility in the Bronze Age eastern Mediterranean. In E. Kiriatzi & C. Knappett (Eds.), *Human mobility and technological transfer in the prehistoric Mediterranean* (pp. 68–93). Cambridge University Press. https://doi.org/10.1017/9781316536063.006

Bieniawski, Z. T. (1989). *Engineering rock mass classifications*. Wiley.

Brilli, M., Giustini, F., & Barone, P. M. (2018). Characterizing the Alabastro Lisato or Fiorito of Hierapolis in Phrygia: A simple method to identify its provenance using carbon stabe isotopes. *Archaeometry*, *3*, 403–418. https://doi.org/10.1111/arcm.12315

De Kock, T., De Boever, W., Dewanckele, J., Boone, M. A., Jacobs, P., & Cnudde, V. (2015). Characterization, performance and replacement stone compatibility of building stone in the 12th century tower of Dudzele (Belgium). *Engineering Geology*, *184*, 43–51. https://doi.org/10.1016/j.enggeo.2014.10.026

Djurić, B. (2019). The logistics behind ancient art, The case of Noricum and Pannoniae. In B. Porod & P. Scherrer (Eds.), *Internationalen Kolloquiums Zum Provinzialrömischen Kunstschaffen Der Stifter Und Sein Monument Gesellschaft* (pp. 8–38). Universität Graz.

Dujardin, L. (2004). Le commerce de la pierre à bâti en Normandie (époques médiévale et moderne). In G. Gosset & J. Leroy (Eds.), *Matériau et Construction en Normandie du Moyen Âge à nos jours* (pp. 151–159). Société d'archéologie et d'histoire de la Manche.

Dujardin, L. (2006). L'utilisation de la pierre dans la construction rurale en Normandie aux époques médiévale et moderne. *In Situ*, *7*. https://doi.org/10.4000/insitu.2746

Entwisle, D., Lee, K. A., & Lawley, R. S. (2015). *User guide for 'BGS civils': a suite of engineering properties datasets (open report OR/15/065)*. British Geological Survey.

Fish, L. (2001). Computer modelling of cave passages. *Compass Tape*, *15*, 19–24.

Fort, R., Chapa, T., & González Reyero, S. (2019). Selective use of limestone in Iberian iron age sculptures and monuments: A case study from Jutia (Albacete, Spain). *Archaeological and Anthropological Sciences*, *11*, 853–870. https://doi.org/10.1007/s12520-017-0574-6

Freccero, A. (2015). Marble trade in antiquity: Looking at Labraunda. *Anatolia Antique*, *23*, 11–54. https://doi.org/10.4000/anatoliaantiqua.344

Fronteau, G., Moreau, C., Thomachot-Schneider, C., & Barbin, V. (2010). Variability of some Lutetian building stones from the Paris Basin, from characterisation to conservation. *Engineering Geology*, *115*, 158–166. https://doi.org/10.1016/j.enggeo.2009.08.001

Frumkin, A., Bar-Matthews, M., Davidovich, U., Langford, B., Ullman, M., & Zissu, B. (2014). In-situ dating of ancient quarries and the source of flowstone ('calcite-alabaster') artifacts in the southern Levant. *Journal of Archaeological Science*, *41*, 749–758. https://doi.org/10.1016/j.jas.2013.09.025

Gao, B., Zhang, H., Yang, Z., Fu, Y., & Luo, L. (2019). The development mechanism and control technology visualization of the vault cracks in the ancient underground cavern of Longyou. *Episodes*, *42*, 287–299. https://doi.org/10.18814/epiiugs/2019/019023

He, W. T., Yang, Z. F., Lin, J., Wang, J. Y., & Luo, Q. H. (2016). A preliminary stability analysis of a cavern complex at Changyu quarry, China. In Z. Yang & C. Tanimoto (Eds.), *Ancient underground opening and preservation* (pp. 55–61). Taylor & Francis.

Hellstrom, J. (2006). U–Th dating of speleothems with high initial ^{230}Th using stratigraphical constraint. *Quaternary Geochronology*, *1*, 289–295. https://doi.org/10.1016/j.quageo.2007.01.004

Hoyez, B. (2008). *Les Falaises du Pays de Caux: Lithostratigraphie des craies turono-campaniennes*. Publications des Universités de Rouen et du Havre.

Hyslop, E., McMillan, A., Cameron, D., Leslie, A., & Lott, G. (2010). Building stone databases in the UK: A practical resource for conservation. *Engineering Geology*, *115*, 143–148. https://doi.org/10.1016/j.enggeo.2009.05.008

Klemm, A., & Wiggins, D. (2016). In J. M. Khatib (Ed.), *Sustainability of natural stone as a construction material, in: Sustainability of construction materials* (pp. 283–308). Elsevier/Woodhead. https://doi.org/10.1016/b978-0-08-100370-1.00012-3

Korkanç, M. (2018). Characterization of building stones from the ancient Tyana aqueducts, Central Anatolia, Turkey: Implications on the factors of deterioration processes. *Bulletin of Engineering Geology and the Environment*, *77*, 237–252. https://doi.org/10.1007/s10064-016-0930-2

Lardin, P. (1998). *Les chantiers du bâtiment en Normandie orientale (XIV–XVe siècles): Les matériaux et les hommes*. Presses du Septentrion.

Lardin, P. (2016). Les relations des ports du littoral de la Basse-Seine et de Rouen avec leurs hinterlands à la fin du Moyen Âge. *Revue Belge de Philologie et d'Histoire*, *94*, 959–971. https://doi.org/10.3406/rbph.2016.8911

Lasseur, E., Guillocheau, F., Robin, C., Hanot, F., Vaslet, D., Coueffe, R., et al. (2009). A relative water-depth model for the Normandy chalk (Cenomanian–middle Coniacian, Paris Basin, France) based on facies patterns of metre-scale cycles, *Sedimentary Geology*, *213*, 1–26. https://doi.org/10.1016/j.sedgeo.2008.10.007

Mileusnić, M., Maričić, A., & Hruškova Hasan, M. (2019). Croatian geological heritage related to historical mining and quarrying. *European Geologist Journal*, *48*, 5–9.

Mortimore, R. (2011). A chalk revolution: What have we done to the chalk of England? *Proceedings of the Geological Association*, *122*, 232–297. https://doi.org/10.1016/j.pgeola.2010.09.001

Mortimore, R. N. (2019). Late Cretaceous to Miocene and quaternary deformation history of the chalk: Channels, slumps, faults, folds and glacitectonics. *Proceedings of the Geological Association*, *130*, 27–65. https://doi.org/10.1016/j.pgeola.2018.01.004

Nehme, C., Farrant, A., Ballesteros, D., Todisco, D., Rodet, J., Sahy, D., et al. (2020). Reconstructing fluvial incision rates based upon palaeo-water tables in chalk karst networks along the seine valley (Normandy, France). *Earth Surface Processes and Landforms*, *45*(8), 1860–1876. https://doi.org/10.1002/esp.4851

Orbons, J. (2018). GIS visualisation and analyses of underground stone quarries. In *Virtual archaeology (from air, on earth, under water and at museum)* (pp. 152–162). The State Hermitage Publishers. https://doi.org/10.1145/585026.585030

Perrotti, M., Lollino, P., Luciano Fazio, N., & Parise, M. (2019). Stability charts based on the finite element method for underground cavities in soft carbonate rocks: Validation through case-study applications. *Natural Hazards and Earth System Sciences*, *19*, 2079–2095. https://doi.org/10.5194/nhess-19-2079-2019

Pivko, D. (2017). Jurassic red nodular limestone from NE Slovakia used as the Ľubovňa 'marble' during the Renaissance in Slovakia and Poland. *Geological Quarterly*, *61*(1), 53–61. https://doi.org/10.7306/gq.1303

Pivko, D. (2018). Extraction methods in historical quarries in Slovakia and nearby areas for dressed stone products. *Acta Geologica Slovaca*, *10*, 105–131.

Pons-Branchu, E., Douville, E., Roy-Barman, M., Dumont, E., Branchu, P., Thil, F., et al. (2014). A geochemical perspective on Parisian urban history based on U–Th dating, laminae counting and yttrium and REE concentrations of recent carbonates in underground aqueducts. *Quaternary Geochronology*, *24*, 44–53. https://doi.org/10.1016/j.quageo.2014.08.001

Quesnel, F., Couëffé, R., Duriez, M., & Lasseur, E. (2008). *Carte géologique harmonisée du département de la Seine-Maritime, Notice technique 118*. Bureau de Recherches Géologiques et Minières.

Romana, M. (1993). A geomechanical classificaton for slopes. In J. Hudson (Ed.), *Comprehensive rock engineering* (pp. 575–600). Pergamon Press. https://doi.org/10.1016/B978-0-08-042066-0.50029-X

Roy-Barman, M., & Pons-Branchu, E. (2016). Improved U–Th dating of carbonates with high initial ^{230}Th using stratigraphical and coevality constraints. *Quaternary Geochronology*, *32*, 29–39. https://doi.org/10.1016/j.quageo.2015.12.002

Rožič, B., Gale, L., Brajković, R., Popit, T., & Žvab Rožič, P. (2018). Lower Jurassic succession at the site of potential Roman quarry Staje near Ig (Central Slovenia). *Geologija*, *61*, 49–71. https://doi.org/10.5474/geologija.2018.004

Russell, B. (2017). Stone quarrying in Greece: Ten years of research. *Archaeological Reports*, *63*, 77–88. https://doi.org/10.1017/S0570608418000078

Scotto di Santolo, A., Evangelista, L., & Evangelista, A. (2015). Analysis of the stability of a rock cavern: The Fontanelle Cemetery. In G. Lollino, D. Giordan, C. Marunteanu, B. Christaras, I. Yoshinori, & C. Margottin (Eds.), *Engineering geology for society and territory*, (Vol. 8, pp. 47–51). Springer. https://doi.org/10.1007/978-3-319-09408-3_5

Shawarby, A., Fathy, E., & Sadek, M. (2009). National inventory and database of ancient stone-quarry landscapes in Egypt. *Geological Survey of Norway Special Publication*, *12*, 155–163.

Shekofteh, A., Oudbashi, O., Cultrone, G., & Ansari, M. (2020). Geochemical and petrographic identification of stone quarries used for the construction of the Anahita Temple of Kangavar (West Iran). *Heritage Science*, *8*, 14. https://doi.org/10.1186/s40494-020-0361-z

Shtober-Zisu, N., & Zissu, B. (2018). Lithology and the distribution of early Roman-era tombs in Jerusalem's necropolis. *Progress in Physical Geography*, *42*, 628–649. https://doi.org/10.1177/0309133318776484

Sibout, P. (2011). La longue histoire des carrières de Caumont. *Études Normandes*, *60*, 27–36. https://doi.org/10.3406/etnor.2011.2875

Storemyr, P., & Heldal, T. (2017). Reconstructing a medieval underground soapstone quarry: Bakkaunet in Trondheim in an international perspective. In G. Hansen & P. Storemyr (Eds.), *Soapstone in the north quarries, products and people 7000 BC – AD 1700* (pp. 107–132). University of Bergen.

Tomat, A. (2009). La pierre en vallée de Seine de Vernon au Havre. *Études Normandes*, *58*, 15–20. https://doi.org/10.3406/etnor.2009.1771

Trimmis, K. (2018). Paperless mapping and cave archaeology: A review on the application of DistoX survey method in archaeological cave sites. *Journal of Archaeological Science: Reports*, *18*, 399–407. https://doi.org/10.1016/j.jasrep.2018.01.022

Turmel, A., Fronteau, G., Chalumeau, L., Deroin, J. P., Eyssautier-Chuine, S., Thomachot-Schneider, C., et al. (2016). GIS-based variability of building materials towards the Île-de-France cuesta (Paris Basin, France): Inventory, distribution, uses and relationship with the environment. *Geological Society Special Publication*, *416*, 113–131. https://doi.org/10.1144/SP416.16

Tziligkaki, E. K., & Stamatakis, M. (2016). Underground quarries in the area of Agiades, Samos Island, Greece: Notes on historical topography and chronology. *Bulletin of the Geological Society of Greece*, *53*, 161–192. https://doi.org/10.12681/bgsg.18835

Van Lint, J., Giot, D., & Callec, Y. (2003). *Carte géologique harmonisée du département de l'Eure*. Bureau de Recherches Géologiques et Minières.

Webber, N. (2005). *The evolution of Norman Identity* (pp. 911–1154). Boydell Press, Woodbridge.

Wilson, A., & Bowman, A. (2018). *Trade, commerce and the state in the Roman world*. Oxford University Press.

Zaid, S. M., Elbadry, O., Ramadan, F., & Mohamed, M. (2015). Petrography and geochemistry of pharaonic sandstone monuments in tall san Al Hagr, Al Sharqiya governorate, Egypt: Implications for provenance and tectonic setting. *Turkish Journal of Earth Sciences*, *24*, 344–364. https://doi.org/10.3906/yer-1407-20

SUPPORTING INFORMATION

Additional supporting information may be found in the online version of the article at the publisher's website.

How to cite this article: Ballesteros, D., Nehme, C., Roussel, B., Delisle, F., Pons-Branchu, E., & Mouralis, D. (2022). Historical underground quarrying: A multidisciplinary research in the Caumont quarry (c. 13th–19th centuries), France. *Archaeometry*, *64*(4), 849–865. https://doi.org/10.1111/arcm.12758